

Effects of different stocking densities on tracheal barrier function and its metabolic changes in finishing broilers

Yuanyuan Wang, Dianchun Wang, Jiangshui Wang, Kaixuan Li, Chianning Heng, Lei Jiang, Chenhao Cai, and Xiuan Zhan¹

College of Animal Sciences, Zhejiang University, Hangzhou, China

ABSTRACT In the present study, we evaluated the effects of various stocking densities on the tracheal barrier and plasma metabolic profiles of finishing broilers. We randomly assigned 1,440 Lingnan Yellow feathered broilers (age 22 d) to 5 different stocking density groups (8 m⁻², 10 m⁻², 12 m⁻², 14 m⁻², and 16 m⁻²). Each of these consisted of 3 replicates. The interleukin (IL)-1 β and IL-10 concentrations were substantially higher in the 16 m⁻² treatment group than they were in the 8 m⁻² and 10 m⁻² treatment groups ($P < 0.05$). Nevertheless, IL-4 did not significantly differ among the 5 treatments ($P > 0.05$). The tracheal mucosae of the birds in the 16 m⁻² group (high stocking density, **HSD**) were considerably thicker than those for the birds in the 10 m⁻² group (control, **CSD**). Relative to CSD, the claudin1 expression level was lower, and the muc2 and

caspase3 expression levels were higher for HSD. Compared with CSD, 10 metabolites were significantly upregulated ($P < 0.05$), and 7 were significantly downregulated ($P < 0.05$) in HSD. Most of these putative diagnostic biomarkers were implicated in matter biosynthesis and energy metabolism. A metabolic pathway analysis revealed that the most relevant and critical biomarkers were pentose and glucuronate interconversions and the pentose phosphate pathway. Activation of the aforementioned pathways may partially counteract the adverse effects of the stress induced by high stocking density. This work helped improve our understanding of the harmful effects of high stocking density on the tracheal barrier and identified 2 metabolic pathways that might be associated with high stocking density-induced metabolic disorders in broilers.

Key words: broiler, immunity, metabolomics, stocking density, tracheal barrier

2020 Poultry Science 99:6307–6316

<https://doi.org/10.1016/j.psj.2020.09.026>

INTRODUCTION

Broiler stocking density is usually expressed in terms of the number of housed birds or kilograms live weight per square meter of floor space at depopulation or the end of growing period (Meluzzi and Sirri, 2009). Stocking density may have critical implications for poultry production (Simsek et al., 2009). Profitability per unit space increases with stocking density. Hence, appropriate increases in stocking density are expected in poultry production. However, excessively high stocking density has negative consequences for poultry production and welfare (Mitchell and Kettlewell, 1998; Wang et al., 2019). In broilers, these include reductions in growth performance, feed utilization, carcass traits,

and immunity (Houshmand et al., 2012), enhanced physiological and oxidative stress, and intestinal mucosal injury (Mashaly et al., 1984; Li et al., 2019).

Bird crowding raises litter temperature, elevates moisture and nitrogen content, dissipates increases in metabolic heat, and enhances microbial activity (Meluzzi and Sirri, 2009). Poor litter quality adversely affects the ambient environment by elevating dust and ammonia levels and humidity which may, in turn, lead to respiratory problems (Meluzzi and Sirri, 2009; Abudabos et al., 2013). It is the respiratory tract that first enters into contact with inhaled pathogens (Pizzolla et al., 2017). Its mucous membrane is the first line of defense against the invasion of exotic microbial pathogens. Therefore, the immune function of the tracheal mucosa plays an integral part in resistance to adverse stimuli (Fan et al., 2015).

Metabolomics is an emerging research area that uses high-throughput techniques to quantitate small-molecule metabolites in biological samples (Wang et al., 2018a). Identification and integrative analysis of these metabolites may comprehensively characterize

© 2020 Published by Elsevier Inc. on behalf of Poultry Science Association Inc. This is an open access article under the CC BY-NC-ND license (<http://creativecommons.org/licenses/by-nc-nd/4.0/>).

Received May 22, 2020.

Accepted September 3, 2020.

¹Corresponding author: xazan@zju.edu.cn

molecular and cellular metabolism under various physiological conditions (Fiehn, 2001). Therefore, metabolomics can elucidate metabolic alterations in biological systems and nutritional intervention mechanisms via pathways integrated with related metabolites (Ibero-Baraibar et al., 2016). Several studies have investigated growth performance, antioxidant capacity, and physiological stress. However, most of them evaluated only a narrow range of bird stocking densities and reported a wide range of inconsistent conclusions. To the best of our knowledge, there are few, if any, studies that have used gas chromatography tandem time-of-flight mass spectrometry to analyze the impact of stocking density. Here, the relative effects of 5 broiler stocking densities in the range of 8–16 m⁻² on tracheal barrier function were assessed. In addition, we identified the metabolic phenotypes associated with high stocking density and linked to broiler growth and health status.

MATERIALS AND METHODS

All procedures herein were conducted in accordance with the Chinese Guidelines for Animal Welfare and approved by the Zhejiang University Institutional Animal Care and Use Committee (ZJU 2018-480-12).

Chickens, Diet, and Management

Bird experiments and treatments were performed in accordance with our previously described methods (Cai et al., 2019). A local commercial hatchery was the source of 1,530 Lingnan Yellow broiler chickens aged 1 d. Throughout the experiment, the birds were housed in 15 concrete floor rooms each 8 m² in area and bedded with a 6-cm layer of rice hulls. During a 21-d pre-experiment, the birds were reared at a stocking density of 12.75 m⁻². Sick and weak chicks were removed during this period. On day 22, One hundred four hundred forty broilers (equal numbers of males and females) similar in weight were randomly assigned to 5 different treatments of which each had 3 replicates. All rooms were replenished with fresh rice hulls. The stocking densities were 8 m⁻², 10 m⁻², 12 m⁻², 14 m⁻², and 16 m⁻² or 64, 80, 96, 112, and 128 birds per room, respectively. All birds had *ad libitum* access to feed and water throughout the experimental period and were subjected to 2L-1D light-dark cycles per day. A corn–soybean meal basal diet was formulated to meet the NRC nutrient requirements (1994) (Table 1). For all rooms, temperature and relative humidity were fixed at 25°C and 55 ± 5%, respectively.

Sample Collection and Processing

At 50 d, twelve male broilers (4 per replicate) were randomly selected from each treatment. The feed was withdrawn 12 h before slaughter, but the birds still had *ad libitum* water access. Blood samples (5 mL bird⁻¹) were taken from the vein under the wing, collected in a coagulant tube, and centrifuged at 3,000 g and 4°C for 10 min to obtain sera that were

then stored at –80°C until the subsequent analyses. The birds were then electrically stunned, exsanguinated, and dissected by a trained team to collect tissue samples. The upper 0.5 cm of the tracheal walls were fixed in 4% (v/v) paraformaldehyde, and the mucosae of the other tracheal segments were gently scraped and stored at –80°C until the subsequent analyses.

Trachea Morphology

Samples of the tracheal walls from birds stocked at 8 m⁻² and 16 m⁻² were preserved in formaldehyde and processed for histological examination. The tracheal samples were dehydrated, embedded in paraffin wax, and sliced into 5-μm sections on a rotary microtome. The sections were then stained with hematoxylin and eosin for morphological analysis and digitally photographed under a light microscope (Olympus, Tokyo, Japan).

Determination of Relative Protein Expression Using Western Blotting

The tracheal expression levels of claudin1, muc2, and caspase3 were determined using Western blotting. Total protein extraction was performed with T-PER Tissue Protein Extraction Reagent (No. 78510; Thermo Fisher Scientific, Waltham, MA). Proteins were then quantified with a bicinchoninic acid (bicinchoninic acid) Quantitation Kit. SDS-PAGE and membrane transfer were conducted, and TBST containing 5% (w/v) non-fat dry milk or bovine serum albumin was added to the membrane to block it at room temperature for 1 h. Antibody (1:100) (Beyotime Biotechnology) was added, and the membrane was incubated overnight at 4°C and washed. Secondary antibody (goat anti-mouse IgG [H + L]) (Beyotime Biotechnology) was added and incubated at room temperature for 1 h, and the membrane was washed. SuperSignal West Dura Extended Duration Substrate (Thermo Fisher Scientific) was used for Western blot detection. The optical densities of the bands were measured with Image J software (National Institute of Health, Bethesda, MD). β-actin was the internal control. The relative abundance of each target protein was expressed as the ratio of target protein to β-actin.

Determination of Immune Status

Commercial kits for all cytokine indices were purchased from the Nanjing Jiancheng Bioengineering Institute, Nanjing, China. One gram tracheal mucosa was homogenized in 9 mL of 0.9% (w/v) sterile normal saline on ice and centrifuged at 3,500 × g and 4°C for 15 min. Total protein in the tissue supernatant was measured with a BCA protein assay kit (Pierce, Rockford, IL) according to the manufacturer's protocol. The tissue supernatant was stored at –80°C and used for enzyme-linked immunosorbent assay. The tracheal mucosa supernatant was analyzed for interleukin (IL)-1β, IL-4, and IL-10 according to the assay kit instructions.

Table 1. Composition and nutrient level of the basal diet used in different phases of trial (% air-dry basis).

Items	Starter (1–21 d)	Grower (22–42 d)	Finisher (43–60 d)
Ingredients, %			
Corn	58.00	35.50	33.50
Sorghum	-	16.00	17.00
Barley	-	10.00	13.00
Soybean meal	34.00	19.70	15.70
Corn gluten meal	2.00	5.80	5.30
DDGS ³	-	5.00	8.00
Lard	-	4.00	3.70
Soybean oil	1.80	-	-
NaCl	0.40	0.30	0.30
CaHPO ₄	1.30	1.00	1.00
Limestone	1.40	1.20	1.20
Zeolite	0.10	0.50	0.30
Premix ¹	1.00	1.00	1.00
Total	100.00	100.00	100.00
Nutrient levels ² (%)			
ME (MJ/kg)	12.10	12.93	12.92
CP	22.94	21.63	19.63
Lys	1.25	1.03	0.90
Met	0.56	0.47	0.44
Met + Cys	0.90	0.78	0.74
Calcium	1.12	0.94	0.98
Total phosphorus	0.63	0.52	0.52

¹The Premix provides per kg of diet: Fe 75 mg, Cu 10 mg, Zn 95 mg, Mn 110 mg, I 0.35 mg, Se 0.30 mg, V_A 9,600IU, V_{D3} 2,700IU, V_E 36 mg, V_{K3} 3 mg, V_{B1} 3 mg, V_{B2} 10.5 mg, V_{B6} 4.20 mg, V_{B12} 0.03 mg, nicotinamide 60 mg, D-calcium pantothenate 18 mg, folic acid 1.5 mg, D-biotin 0.225 mg, choline, 500 mg.

²ME is a calculated value; other nutrient levels are measured values.

³DDGS is distillers dried grains with solubles.

Sample Preparation for GC-TOFIMS Analysis

Samples were prepared for the metabolomics analysis as previously described (Dunn et al., 2011). Briefly, 100 µL serum was added to 350 µL extraction liquid (methanol:acetonitrile:water = 2:2:1, v/v/v) and 20 µL *L*-2-chlorophenylalanine. The mixture was maintained at 4°C for 30 min and centrifuged at 13,000 g for 15 min. The supernatant (400 µL) was collected into a 1.5-mL tube, transferred to a glass vial, and dried by vacuum. Methoxyamine salt reagent (methoxyamine HCl dissolved in pyridine, 20 mg mL⁻¹) was added, and the mixture was heated in an oven to 80°C for 30 min, derivatized with *N,O*-bis-(trimethylsilyl)trifluoroacetamide, and incubated at 70°C for 1 h. The final mixture was vortexed for 1 min and used in the subsequent analysis (Li et al., 2018).

GC-TOFIMS Analysis

Based on our previously described methods (Wang et al., 2020), the derivatized samples were analyzed in

an Agilent 7,890 GC System (Agilent Technologies, Santa Clara, CA) fitted with a Pegasus 4D TOFMS (LECO, St. Joseph, MI) and a 30 m × 250 µm i.d. DB-5MS capillary column. The latter had a 0.25-µm film thickness and was coated with 95% dimethylpolysiloxane cross-linked with 5% diphenyl. The initial temperature was maintained at 80°C for 12 s, increased to 180°C at 10°C min⁻¹, then to 240°C at 5°C min⁻¹, and then to 290°C at 20°C min⁻¹ and maintained there for 11 min. One microliter of sample solution was injected, helium was the carrier gas, and the flow rate was 1 mL min⁻¹. The transfer line and ion source temperatures were 245°C and 220°C, respectively. The MS data were acquired in full-scan mode in a mass-to-charge ratio (m/z) range of 20–600.

GC-TOFIMS Data Acquisition and Processing

Raw peak extraction, data baseline filtering and calibration, peak alignment, deconvolution analysis, peak

Table 2. Effects of stocking density on immune status in trachea of finishing broilers.

Items	Stocking density (birds/m ²)					SEM	<i>P</i> -value
	8	10	12	14	16		
IL-1β (ng/g)	0.098 ^c	0.099 ^c	0.120 ^b	0.124 ^b	0.149 ^a	0.004	0.000
IL-4 (ng/g)	0.469	0.484	0.454	0.479	0.460	0.063	0.744
IL-10 (ng/g)	0.298 ^b	0.296 ^b	0.303 ^{ab}	0.334 ^{ab}	0.347 ^a	0.008	0.102

^{a-c}Means within a row with not common superscripts significantly differ (*P* < 0.05).

Each value is the mean, n = 12.

Abbreviations: IL-1β, interleukin-1β; IL-4, interleukin-4; IL-10, interleukin-10.

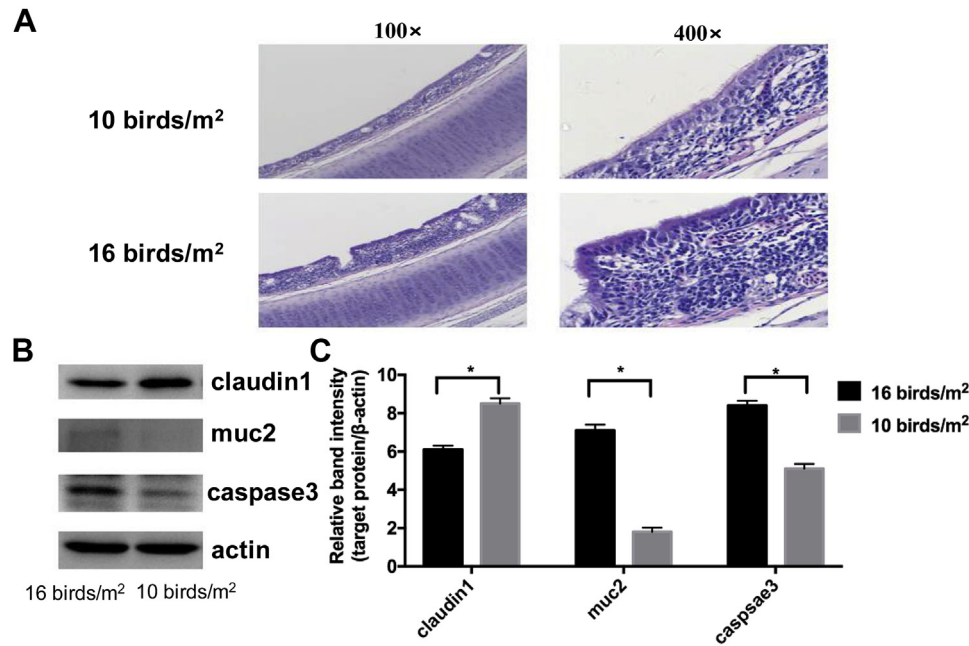


Figure 1. Effect of stocking density in trachea on finishing broilers. (A) Representative H&E-stained images; (B) Expression of claudin1, muc2, and caspase3 in trachea tissue were determined by Western blot. (C) Relative changes in the density of claudin1, muc2, and caspase3 were analyzed. Data presented as relative band intensity of claudin1, muc2, and caspase3 to β -actin. Values are means, with their SDs represented by vertical bars. (* $P < 0.05$). Each value is the mean, $n = 3$.

identification, and peak area integration were performed using Chroma TOF v. 4.3X and the LECO-Fiehn Rtx5 database (LECO). Peak identification was tested by the retention time index method. Missing data were filled in using half the minimum value and a numerical simulation method. Data noise was filtered out according to an interquartile range and normalized by area normalization methods. SIMCA v. 14.1 (Umetrics,

Umea, Sweden) performed multivariate variable pattern recognition analyses comprising principal component analysis (PCA), partial least squares discriminant analysis, and orthogonal partial least-squares discriminant analysis (OPLS-DA). The PCA showed the internal data structure and displayed both similarities and differences. The OPLS-DA further enhanced group separation and clarified the variables. The R^2Y and Q^2 were applied

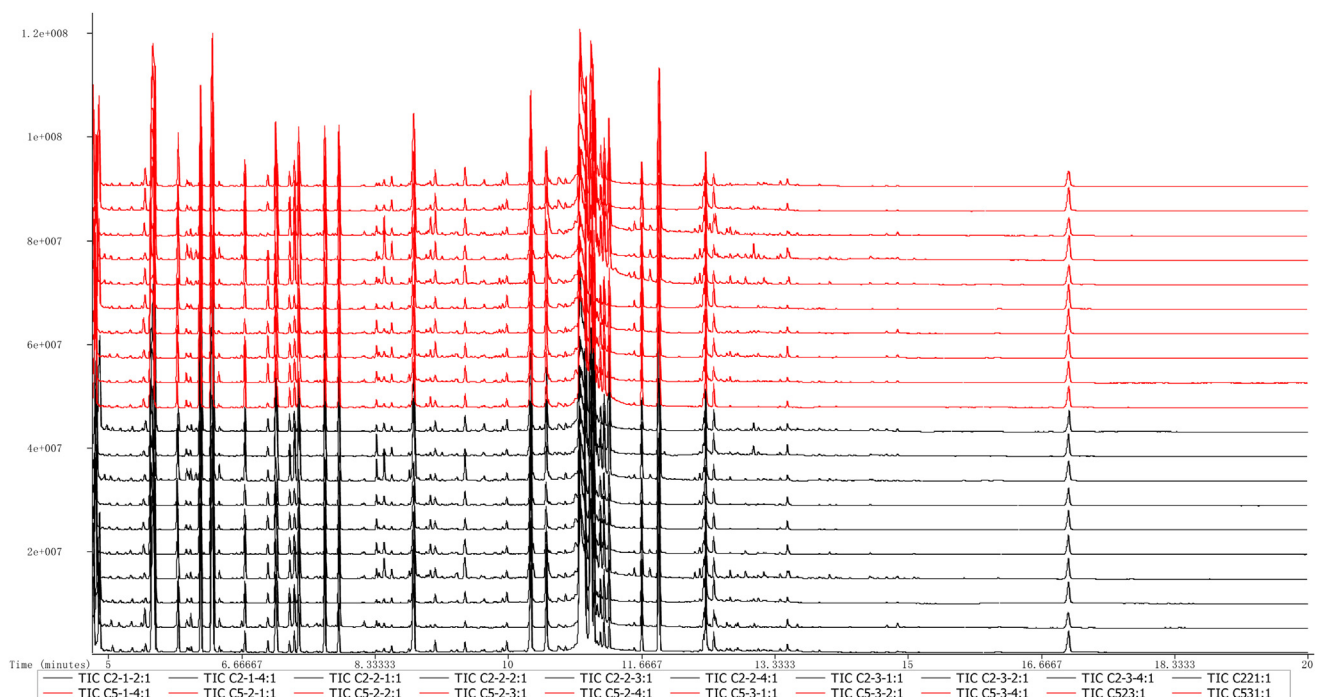


Figure 2. Total GC-TOF/MS ion flow about metabolites in the broilers' serum.

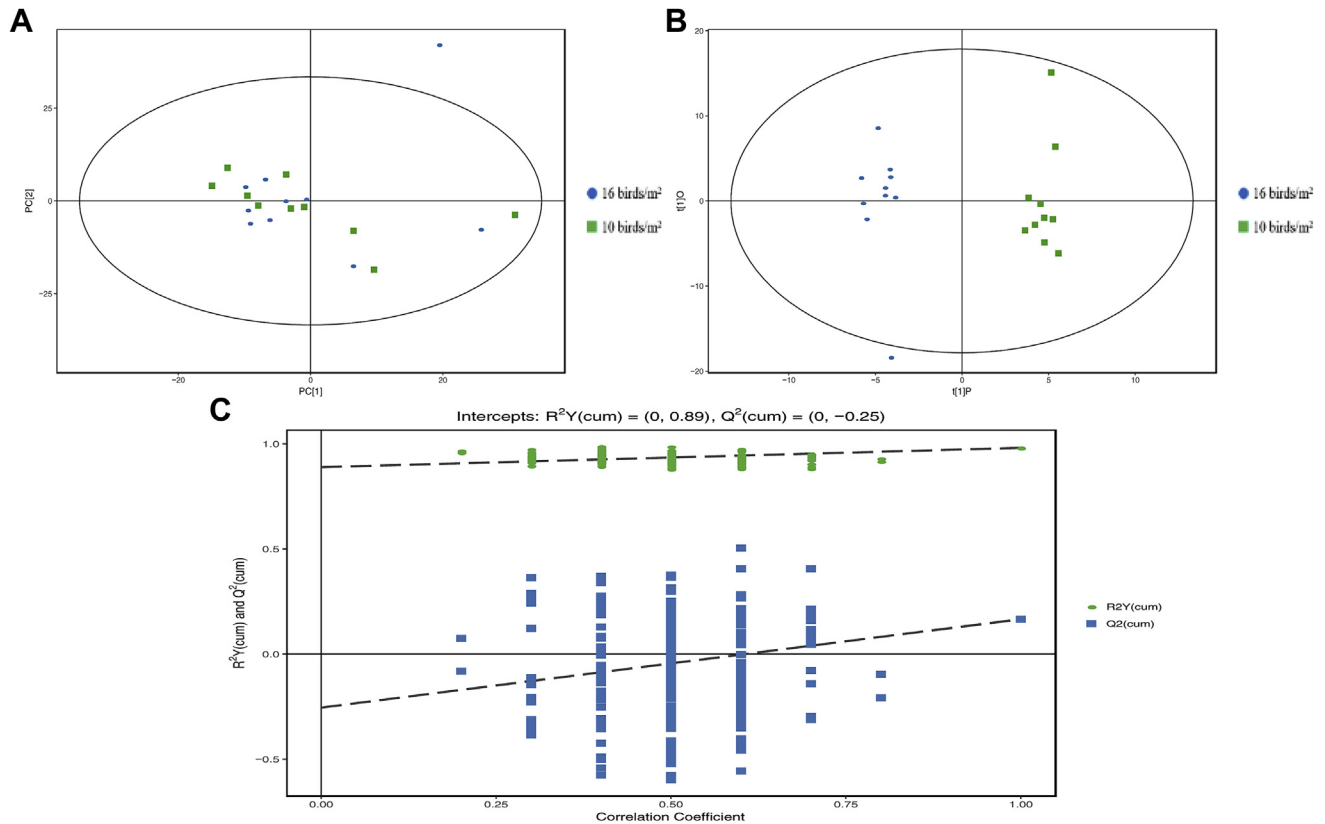


Figure 3. (A) Principal component analysis (PCA) score plots, (B) orthogonal projections to latent structure-discriminant analysis (OPLS-DA) score plots ($R^2X = 0.0$, $R^2Y = 0.089$, $Q^2 = -0.25$), and (C) permutation test of OPLS-DA from the LC-TOF/MS metabolite profiles of plasma for 16 birds/m² vs. group 10 birds per m². Blue circle: 16 birds per m²; green square: 10 birds per m²; Green circle: R^2 ; blue square: Q^2 . The dash line represents the regression line for R^2 and Q^2 .

to evaluate the model predictive ability and fitting level. The metabolites responsible for differentiating both groups were filtered under the following conditions: variable importance in the projection > 1 , $P \leq 0.05$ (threshold), and 95% Hotelling's T-squared ellipse (Wang et al., 2020).

Statistical Analysis

Data were subjected to one-way ANOVA in SPSS v. 19.0 (IBM Corp., Armonk, NY) and expressed as means plus SEM. Differences between treatment means were examined by Duncan's multiple range tests. A $P < 0.05$ indicated statistical significance. Student t test identified differences between both groups in terms of their metabolite levels.

RESULTS

Immune Status

Table 2 shows that both the IL-1 β and IL-10 concentrations significantly increased as the stocking density increased from 8 m⁻² to 16 m⁻² ($P < 0.05$). In contrast, there were no significant differences among stocking densities in terms of IL-4 content ($P > 0.05$). The IL-1 β and IL-10 concentrations in the birds stocked at 16 m⁻² were

significantly higher than those stocked at 8 m⁻² and 10 m⁻² ($P < 0.05$).

Immune System and Tracheal Barrier Function

Digital images of hematoxylin and eosin-stained sections indicated that the birds stocked at 10 m⁻² (control group, CSD) presented with normal tracheal morphology. However, the tracheae of the birds stocked at 16 m⁻² (high stocking density group, HSD) were thicker than those of the CSD group. In the HSD group, the mucosal surfaces were fragmented, the submucosae were thickened, and relatively more goblet and ciliated cells were visible under high magnification (400 \times) (Figure 1A). To explore the effects of HSD on tracheal barrier function, the relative protein expression levels of claudin1, muc2, and caspase3 in the tracheal tissue were measured. Relative to CSD, HSD presented with markedly lower claudin1 expression but higher muc2 and caspase3 expression (Figures 1B and 1C).

Metabolic Differences in the Sera of the 16 m⁻² and 10 m⁻² Treatment Groups

Total Gas Chromatography Time-of-Flight Mass Spectrometry (GC-TOF/MS) ion chromatograms

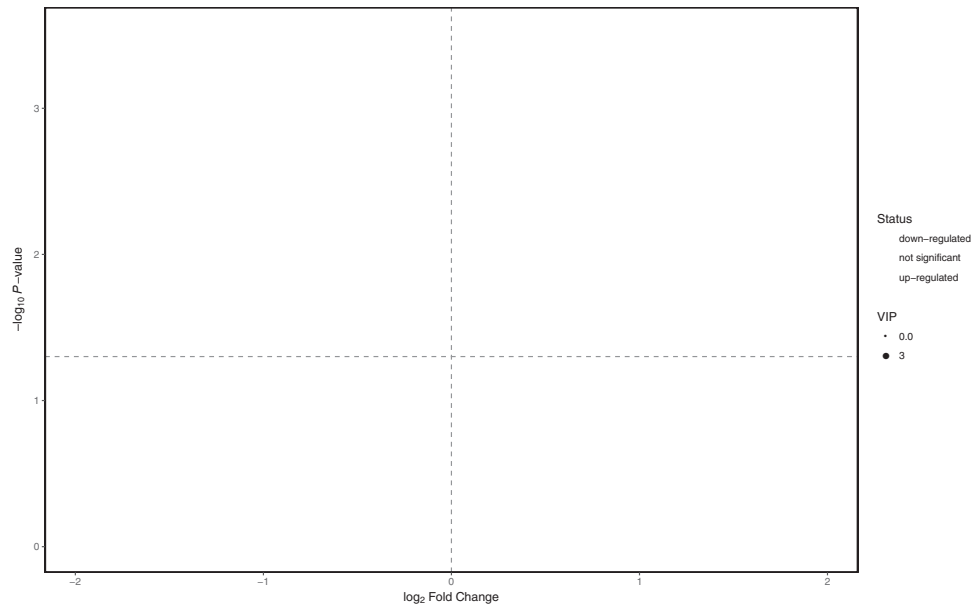


Figure 4. Volcano plots of metabolites in serum between 16 birds per m² and 10 birds per m² treatment groups. Each dot represents a metabolite. The larger dots indicate higher variable importance in the projection (VIP) values. The abscissa and ordinate represent the fold change and *P*-value of biomarkers, respectively. The increased and decreased ($P < 0.05$) biomarkers in the treatment group are represented by the red and blue dots, respectively, whereas the gray dots represent the unchanged ($P > 0.05$) metabolites between these 2 groups.

acquired by ultra performance liquid chromatography/tandem mass spectrometry for HSD and CSD are shown in Figure 2. Following pretreatment, standardization with MZmine 2.0 and extraction ion chromatography, 425 integral peaks were detected in the quality control samples, and 629 peaks were identified in the test samples.

The serum samples from the HSD and CSD treatment groups were analyzed on multiple MS platforms to elucidate the relative changes in serum metabolome. The PCA revealed that HSD and CSD broilers were clearly separated on the scores plot (Figure 3A). The PCA also disclosed all outliers or observations located outside

the 95% confidence region of the model. The OPLS-DA elucidated the various metabolic patterns. Figure 3B shows distinctly separated clusters between HSD (blue circle) and CSD (green square). R^2X , Q^2 , and the permutation test results confirmed that the sample quality was acceptable (Figure 3C).

Here, we determined the differentially expressed metabolites primarily responsible for separating HSD and CSD. The potential biomarkers distinguishing HSD and CSD were visualized with a volcano plot (Figure 4). Seventeen serum metabolite biomarkers with similarity >600, variable importance in the projection >1, and $P < 0.05$ were filtered. They comprised mainly lipids, amino acids, carbohydrates, organic acids, amines, and other compounds and were involved in multiple biochemical processes. The biomarkers included 6-phosphogluconic acid, threonic acid, xylitol, benzoic acid, heptadecanoic acid, threonine, halostachine, indole-3-acetic acid, dioctyl phthalate, salicin, uric acid, 2,3-dihydropyridine, conduritol b epoxide, glucoheptonic acid, 3-(1-pyrazolyl)-*L*-alanine, cystine, and 4-acetamidobutyric acid (Table 3). Compared with CSD, the concentrations of 10 metabolites were significantly higher ($P < 0.05$), whereas those of 7 other metabolites were significantly lower ($P < 0.05$) in HSD. Four candidate metabolites (6-phosphogluconic acid, threonic acid, salicin, and 3-(1-pyrazolyl)-*L*-alanine) were selected as biomarkers as they exhibited high sensitivity, specificity, and accuracy in diagnosing broilers under high stocking density stress ($P < 0.01$). Further research is warranted to evaluate these biomarkers for practical applications and elucidate the physiological mechanisms underlying high stocking density-induced metabolic disorders.

The current study compared various serum metabolites between HSD and CSD and clarified the

Table 3. Serum differential metabolites between 16 birds/m² and 10 birds/m² treatment groups.

Items	Mean		VIP	<i>P</i> -value
	Stocking density (birds/m ²)			
	16	10		
6-Phosphogluconic Acid	6.34E-04	2.05E-03	3.04	0.002
Threonic Acid	2.05E-02	1.52E-02	2.52	0.004
Xylitol	2.08E-02	1.73E-02	2.17	0.025
Benzoic Acid	1.62E-01	3.01E-01	2.08	0.021
Heptadecanoic Acid	6.64E-04	1.05E-03	2.01	0.041
Threonine 2	1.78E-02	5.65E-03	1.99	0.050
Halostachine 2	2.48E-03	1.75E-03	1.96	0.030
Indole-3-Acetic Acid	1.89E-04	5.37E-04	1.95	0.026
Dioctyl Phthalate	3.40E-03	5.18E-03	1.90	0.039
Salicin	1.21E-03	3.69E-03	1.84	0.000
Uric Acid	1.02E-03	2.35E-03	1.84	0.046
2,3-Dihydropyridine	2.40E-03	1.53E-03	1.78	0.048
Conduritol b Epoxide 2	4.85E-01	2.71E-01	1.59	0.015
Glucoheptonic Acid 1	7.61E-03	2.69E-03	1.50	0.044
3-(1-Pyrazolyl)-L-Alanine	3.25E-03	1.94E-03	1.35	0.005
Cystine	9.44E-03	5.56E-03	1.21	0.015
4-Acetamidobutyric Acid 2	2.61E-03	1.82E-03	1.14	0.049

Each value is the mean, $n = 10$.

Abbreviation: VIP, variable importance in the projection.

Table 4. Pathway analysis for 16 birds/m² and 10 birds/m² treatment groups using MetaboAnalyst.

Pathway name	Total ¹	Hits ²	Raw p ³	Impact ⁴
Valine, leucine, and isoleucine biosynthesis	10	1	0.067189	0
Pentose and glucuronate interconversions	17	1	0.1118	0.08333
Pentose phosphate pathway	20	1	0.13033	0.08333
Cysteine and methionine metabolism	27	1	0.17225	0
Glycine, serine, and threonine metabolism	33	1	0.20673	0.04786
Tryptophan metabolism	37	1	0.22901	0
Arginine and proline metabolism	38	1	0.23449	0
Aminoacyl-tRNA biosynthesis	44	1	0.26665	0
Purine metabolism	63	1	0.36073	0

¹Represents the total number of metabolites in the corresponding pathway.

²Represents the actually matched number of metabolites.

³Represents the *P*-values from enrichment analysis.

⁴Represents the impact value calculated from pathway topology analysis. Each value is the mean, n = 10.

pathways in which they participate. Nine enriched pathways displayed impact values at a comprehensive level (Table 4). Pentose and glucuronate interconversions, the pentose phosphate pathway, and glycine, serine, and threonine metabolism presented with pathway impact values greater than the relevance cutoff value of 0.00. Their respective impact values were 0.08, 0.08, and 0.05. When the *P*-values were adjusted by hypergeometric testing for the enrichment analysis, only the pentose and glucuronate interconversions and pentose phosphate pathway showed significant difference ($P < 0.05$). Hence, they were characterized as significantly relevant pathways (Figure 5).

DISCUSSION

According to the European Union, animal welfare has become a priority for European consumers and citizens (Verdes et al., 2020). Consumers expect that animal-related products and particularly food must be prepared with respect for the welfare of the animal (Dawkins et al., 2004; Sanchez et al., 2020). It is known that high stocking density reduces bird welfare. A previous study revealed that stocking densities of 8–10 m⁻² can help mitigate the adverse effects of stocking on broiler growth performance and welfare (Cai et al., 2019).

Severe and/or prolonged stress may impair the immune system (immune organs and hematological values)

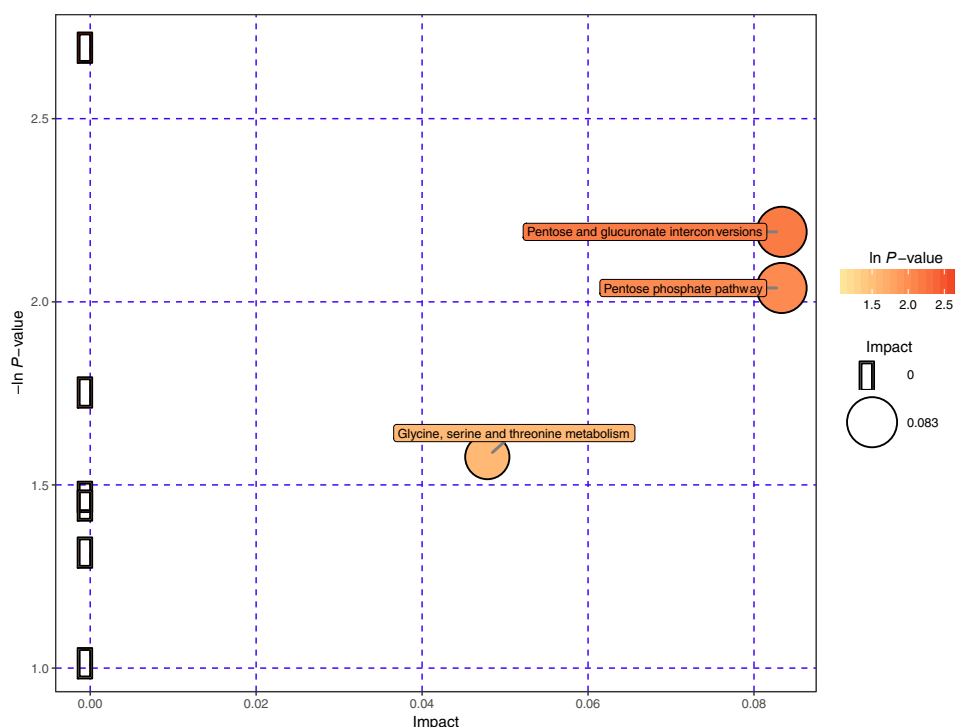


Figure 5. Graphic summary of pathway analysis between 16 birds per m² and 10 birds per m² treatment groups using MetaboAnalyst. The X-axis indicates the pathway impact, and Y-axis represents the pathway enrichment. Larger sizes and darker colors indicate higher pathway enrichment and higher pathway impact values, respectively.

in mature birds (Kang et al., 2011). Therefore, specific immunological factors must be identified and applied to evaluate the stress responses in birds. Immunocytes may be negatively affected by stress (Stevenson et al., 2006) and respond by continuously producing cytokines. However, there has been little research conducted on the influences of bird husbandry stressors on cell-mediated immune indicators such as cytokines. The IL-1 promotes inflammation, whereas IL-4 and IL-10 inhibit it (Hancock et al., 2001). An earlier study reported that IL-1 is continuously secreted when the body is under stress (Appels et al., 2000). Here, tracheal IL-1 and IL-1 β increased with broiler stocking density. The IL-10 is an antiinflammatory cytokine that modulates proinflammatory cytokine suppression (Jolly, 2004). It participates in positive feedback loops involving cytokines and relays negative feedback signals that attenuate activated immune systems after inflammatory triggers (Papadakis and Targan, 2000; Youn et al., 2013). Proinflammatory cytokine overproduction is followed by the onset of immune-mediated inflammation and multiple organ fibroses (Yehudai-Ofir et al., 2020). In contrast, increasing IL-10 production during HSD treatment mitigates inflammation and maintains immunotolerance.

Mucosal integrity and protective protein secretion are vital for efficacious tracheal defense (Su et al., 2019). It is known that intestinal barrier function linearly decreases with increasing stocking density (Goo et al., 2019). To the best of our knowledge, however, there are few if any published reports on the effects of high stocking density on tracheal barrier function. Here, the tracheal structure of CSD had normal morphology whereas that of HSD presented with injured and abnormally thick mucosae after 29 d of high stocking density stimulation. Barrier function may be determined by the integrity of the tight junction between epithelial layers. The tight junction seals apical gaps (Moret  and P rez-Bosque, 2009). Downregulation of tight junction-related genes and proteins may serve as molecular evidence for impaired barrier functions (Gilani et al., 2018). Therefore, we measured selected tight junction-related protein expression in the tracheal mucosa. Claudin-1 is an integral membrane protein localized at the tight junction. It can induce tight junction-like networks in fibroblasts (Inai et al., 1999). Here, we observed substantially downregulated claudin-1 in response to the HSD treatment. The respiratory mucosal epithelium is a barrier against injurious luminal agents such as bacteria, enzymes, and toxins (Wills-Karp, 2000). In this study, we found that HSD presented with markedly increased muc2 protein expression. *MUC* transcription is induced when the airway is exposed to substances such as endotoxin, sulfur dioxide, and allergens that promote mucus secretion (Jany et al., 1991). Normal respiratory epithelium is coated with mucus which has several protective functions. However, mucus hypersecretion is a key symptom of allergic asthma and is associated with airway obstruction and mortality (Wills-Karp, 2000). In addition, caspase induction is an essential step in programmed cell death (apoptosis) (Estrov et al., 1998). The current

study showed that caspase3 expression was considerably higher for HSD than CSD.

To the best of our knowledge, few if any metabolomics experiments have been performed to investigate broiler responses to high stocking densities. A previous study applied metabolomics to disclose altered metabolic patterns in the sera of patients with asthma and identify the mechanisms underlying asthma and its biomarkers (Jung et al., 2013). In the present study, differentially expressed metabolites participated mainly in matter biosynthesis and energy metabolism. Relative to CSD, 10 metabolites were upregulated, whereas 7 others were downregulated in HSD. Xylitol is a five-carbon polyalcohol with numerous applications as a food additive. It is widely distributed in nature (M kinen, 1979). In humans, xylitol is an endogenous metabolite of the uronic acid cycle and an exogenous energy source (Ylikahri, 1979). Xylitol has both food processing and pharmaceutical applications. It is a functional sweetener with prebiotic effects and can lower blood glucose, triglyceride, and cholesterol levels (Ur-Rehman et al., 2015). Threonic acid is a major breakdown product of ascorbic acid metabolism. It is used as a food additive and may have host health benefits (Thomas and Hughes, 1983). It is a major plasma globulin component in poultry, rabbits, and humans (Tenenhouse and Deutsch, 1966). Bhargava et al. (1971) reported that chick antibody titers increased with dietary threonine intake. Decreases in sow plasma IgG were alleviated by threonine supplementation (Cuaron et al., 1984). The foregoing data suggest that threonine participates in immune function. Organic acids such as glucoheptonic and acetamidobutyric acid, amino acids such as alanine and cystine, and other regulatory factors may also benefit host health. Here, we deduced that chronic stress caused by high stocking density triggers alterations in serum metabolite levels which, in turn, help offset the adverse effects of crowding stress.

The aforementioned low molecular weight metabolites are involved in multiple pathways and reactions such as pentose and glucuronate interconversions and the pentose phosphate pathway. Pentose and glucuronate interconversions are implicated in metabolite detoxification and excretion (Fang et al., 2016). A serum metabolic study revealed that *D*-glucuronic acid is associated with pentose and glucuronate interconversions (Sun et al., 2018). The pentose phosphate pathway plays a crucial role in host-parasite relationships. It maintains a pool of NADPI-i which protects against oxidant stress and generates carbohydrate intermediates for biosynthetic pathways of nucleotides and other biochemicals (Barrett, 1997). The pentose phosphate pathway converts glucose-6-phosphate to ribose-5-phosphate which, in turn, is used in nucleotide biosynthesis. The pentose phosphate pathway also generates other important phosphorylated carbohydrates such as erythrose-4-phosphate which is an aromatic amino acid and vitamin precursor. The pentose phosphate pathway produces sedoheptulose-7-phosphate which is a critical component of certain bacterial cell walls (Wood, 1986). NADPH is a hydrogen donor in reductive biosynthesis, and it participates in

xenobiotic detoxification and defense against oxidative stress (Barrett, 1997). In view of influential roles of pentose and glucuronate interconversions and the pentose phosphate pathway, their activation might enable the host to counteract the adverse effects of high stocking density.

Based on the foregoing evidence, it was concluded that broiler tracheal barrier efficacy decreased with increasing stocking density. A metabolomics analysis demonstrated major changes in the serum metabolite profiles of broilers subjected to high stocking density. The modified metabolites induced by high stocking density were involved mainly in energy metabolism. Of these, pentose and glucuronate interconversions and the pentose phosphate pathway were the most relevant and vital. The present study clarified the complex metabolic impact of high stock density on broilers and elucidated the potential mechanisms associated with its negative health effects.

ACKNOWLEDGMENTS

The *financial support* provided by National Key R&D Program of China (project: 2016YFD05005, Beijing, China), Zhejiang Province Key R&D Program of China (project: 2018C02035, Hangzhou, China), China Agriculture Research System (project: CARS-42-G19, Beijing, China) are gratefully acknowledged.

Conflict of Interest Statement: There are no conflicts of interest to declare.

REFERENCES

- Abudabos, A. M., E. M. Samara, E. O. Hussein, M. a. Q. Al-Ghadi, and R. M. Al-Atiyat. 2013. Impacts of stocking density on the performance and welfare of broiler chickens. *Ital. J. Anim. Sci.* 12:e11.
- Appels, A., F. W. Bar, J. Bar, C. Bruggeman, and M. de Baets. 2000. Inflammation, depressive symptomatology, and coronary artery disease. *Psychosom Med.* 62:601–605.
- Barrett, M. 1997. The pentose phosphate pathway and parasitic protozoa. *Parasitol. Today* 13:11–16.
- Bhargava, K., R. Hanson, and M. Sunde. 1971. Effects of threonine on growth and antibody production in chicks infected with Newcastle disease virus. *Poult. Sci.* 50:710–713.
- Cai, C. H., R. X. Zhao, P. Wang, J. S. Wang, K. X. Li, X. A. Zhan, and K. Y. Wang. 2019. Effects of different stocking densities on growth performance, antioxidant ability, and immunity of finishing broilers. *Anim. Sci. J.* 90:583–588.
- Cuaron, J. A., R. P. Chapple, and R. A. Easter. 1984. Effect of lysine and threonine supplementation of sorghum gestation diets on nitrogen balance and plasma constituents in first-litter gilts. *J. Anim. Sci.* 58:631–637.
- Dawkins, M. S., C. A. Donnelly, and T. A. Jones. 2004. Chicken welfare is influenced more by housing conditions than by stocking density. *Nature* 427:342–344.
- Dunn, W. B., D. Broadhurst, P. Begley, E. Zelena, S. Francis-McIntyre, N. Anderson, M. Brown, J. D. Knowles, A. Halsall, and J. N. Haselden. 2011. Procedures for large-scale metabolic profiling of serum and plasma using gas chromatography and liquid chromatography coupled to mass spectrometry. *Nat. Protoc.* 6:1060.
- Estrov, Z., P. F. Thall, M. Talpaz, E. H. Estey, H. M. Kantarjian, M. Andreeff, D. Harris, Q. Van, M. Walterscheid, and S. M. Kornblau. 1998. Caspase 2 and caspase 3 protein levels as predictors of survival in acute myelogenous leukemia. *J. Am. So. Hematol.* 92:3090–3097.
- Fan, X. X., S. Q. Liu, G. H. Liu, J. P. Zhao, H. C. Jiao, X. J. Wang, Z. G. Song, and H. Lin. 2015. Vitamin A Deficiency impairs Mucin expression and Suppresses the mucosal immune function of the respiratory tract in chicks. *Plos. One.* 10:e0139131.
- Fang, H., A. Zhang, J. Yu, L. Wang, C. Liu, X. Zhou, H. Sun, Q. Song, and X. Wang. 2016. Insight into the metabolic mechanism of scoparone on biomarkers for inhibiting Yanghuang syndrome. *Sci. Rep.* 6:37519.
- Fiehn, O. 2001. Combining genomics, metabolome analysis, and biochemical modelling to understand metabolic networks. *Int. J. Genomics.* 2:155–168.
- Gilani, S., G. Howarth, G. Nattrass, S. Kitessa, R. Barekain, R. Forder, C. Tran, and R. Hughes. 2018. Gene expression and morphological changes in the intestinal mucosa associated with increased permeability induced by short-term fasting in chickens. *J. Anim. Physiol. N.* 102:e653–e661.
- Goo, D., J. Kim, H. Choi, G. Park, G. Han, and D. Kil. 2019. Effect of stocking density and sex on growth performance, meat quality, and intestinal barrier function in broiler chickens. *Poult. Sci.* 98:1153–1160.
- Hancock, G. E., C. A. Scheuer, R. Sierzeza, K. S. Pryharski, J. T. McBride, L. F. M. Watelet, P. W. Tebbey, and J. D. Smith. 2001. Adaptive immune responses of patients with asthma to the attachment (G) glycoprotein of respiratory syncytial virus. *J. Infect. Dis.* 184:1589–1593.
- Houshmand, M., K. Azhar, I. Zulkifli, M. Bejo, and A. Kamyab. 2012. Effects of prebiotic, protein level, and stocking density on performance, immunity, and stress indicators of broilers. *Poult. Sci.* 91:393–401.
- Ibero-Baraibar, I., A. Romo-Hualde, C. J. Gonzalez-Navarro, M. A. Zulet, and J. A. Martinez. 2016. The urinary metabolomic profile following the intake of meals supplemented with a cocoa extract in middle-aged obese subjects. *Food Funct.* 7:1924–1931.
- Inai, T., J. Kobayashi, and Y. Shibata. 1999. Claudin-1 contributes to the epithelial barrier function in MDCK cells. *Eur. J. Cell. Biol.* 78:849–855.
- Jany, B., M. Gallup, T. Tsuda, and C. Basbaum. 1991. Mucin gene expression in rat airways following infection and irritation. *Biochem. Bioph. Res. Co.* 181:1–8.
- Jolly, C. A. 2004. Dietary restriction and immune function. *J. Nutr.* 134:1853–1856.
- Jung, J., S. H. Kim, H. S. Lee, G. Choi, Y. S. Jung, D. Ryu, H. S. Park, and G. S. Hwang. 2013. Serum metabolomics reveals pathways and biomarkers associated with asthma pathogenesis. *Clin. Exp. Allergy* 43:425–433.
- Kang, S. Y., Y. H. Ko, Y. S. Moon, S. H. Sohn, and I. S. Yang. 2011. Effects of the Combined stress induced by stocking density and feed restriction on hematological and cytokine Parameters as stress indicators in laying hens. *A-a. J. Anim. Sci.* 24:414–420.
- Li, W., F. Wei, B. Xu, Q. Sun, W. Deng, H. Ma, J. Bai, and S. Li. 2019. Effect of stocking density and alpha-lipoic acid on the growth performance, physiological and oxidative stress and immune response of broilers. *Asian Austral. J. Anim.* 32:1914.
- Li, Y., Y. Guo, Z. Wen, X. Jiang, X. Ma, and X. Han. 2018. Weaning stress Perturbs Gut Microbiome and its metabolic profile in piglets. *Sci. Rep.* 8:18068.
- Mäkinen, K. K. 1979. Xylitol and oral health. *Adv. Food Res.* 25:137–158.
- Mashaly, M. M., M. L. Webb, S. L. Youtz, W. B. Roush, and H. Graves. 1984. Changes in serum corticosterone concentration of laying hens as a response to increased population density. *Poult. Sci.* 63:2271–2274.
- Meluzzi, A., and F. Sirri. 2009. Welfare of broiler chickens. *Ital. J. Anim. Sci.* 8:161–173.
- Mitchell, M., and P. Kettlewell. 1998. Physiological stress and welfare of broiler chickens in transit: solutions not problems! *Poult. Sci.* 77:1803–1814.
- Moretó, M., and A. Pérez-Bosque. 2009. Dietary plasma proteins, the intestinal immune system, and the barrier functions of the intestinal mucosa. *J. Anim. Sci.* 87:E92–E100.
- Papadakis, K. A., and S. R. Targan. 2000. Role of cytokines in the pathogenesis of inflammatory bowel disease. *Annu. Rev. Med.* 51:289–298.

- Pizzolla, A., T. H. Nguyen, J. M. Smith, A. G. Brooks, K. Kedzierska, W. R. Heath, P. C. Reading, and L. M. Wakim. 2017. Resident memory CD8⁺ T cells in the upper respiratory tract prevent pulmonary influenza virus infection. *Sci. Immunol.* 2:eaam6970.
- Sanchez, L. S., I. Blanco-Penedo, J. M. P. Munoz, C. Q. Perez, J. V. Delgado, and J. L. Vega-Pla. 2020. Welfare assessment at a Spanish Army equine Breeding Centre. *Ital. J. Anim. Sci.* 19:137–146.
- Simsek, U., I. Cerci, B. Dalkilic, O. Yilmaz, and M. Ciftci. 2009. Impact of stocking density and feeding regimen on broilers: chicken meat composition, fatty acids, and serum cholesterol levels. *J. Appl. Poult. Res.* 18:514–520.
- Stevenson, L. S., K. McCullough, I. Vincent, D. F. Gilpin, A. Summerfield, J. Nielsen, F. McNeilly, B. M. Adair, and G. M. Allan. 2006. Cytokine and C-reactive protein profiles induced by porcine circovirus type 2 experimental infection in 3-week-old piglets. *Viral. Immunol.* 19:189–195.
- Su, Y., H. Wei, Y. Bi, Y. Wang, P. Zhao, R. Zhang, X. Li, J. Li, and J. Bao. 2019. Pre-cold acclimation improves the immune function of trachea and resistance to cold stress in broilers. *J. Cell. Physiol.* 234:7198–7212.
- Sun, H., A.-h. Zhang, Q. Song, H. Fang, X.-y. Liu, J. Su, L. Yang, M.-d. Yu, and X.-j. Wang. 2018. Functional metabolomics discover pentose and glucuronate interconversion pathways as promising targets for Yang Huang syndrome treatment with Yinchenhao Tang. *Rsc. Adv.* 8:36831–36839.
- Tenenhouse, H. S., and H. Deutsch. 1966. Some physical-chemical properties of chicken γ -globulins and their pepsin and papain digestion products. *Immunochemistry* 3:11–20.
- Thomas, M., and R. Hughes. 1983. A relationship between ascorbic acid and threonic acid in Guinea-pigs. *Food Chem. Toxicol.* 21:449–452.
- Ur-Rehman, S., Z. Mushtaq, T. Zahoor, A. Jamil, and M. A. Murtaza. 2015. Xylitol: a review on bioproduction, application, health benefits, and related safety issues. *Crit. Rev. Food Sci.* 55:1514–1528.
- Verdes, S., Y. Trillo, A. I. Pena, P. G. Herradon, J. J. Becerra, and L. A. Quintela. 2020. Relationship between quality of facilities, animal-based welfare indicators and measures of reproductive and productive performances on dairy farms in the northwest of Spain. *Ital. J. Anim. Sci.* 19:319–329.
- Wang, C., Z. Liu, J. Xue, Y. Wang, X. Huang, and Q. Wang. 2019. Effect of stocking density on growth performance, feather quality, carcass traits, and Muscle chemical component of geese from 49 to 70 Days of age. *J. Appl. Poult. Res.* 28:1297–1304.
- Wang, W., Z. Li, L. Gan, H. Fan, and Y. Guo. 2018a. Dietary supplemental *Kluyveromyces marxianus* alters the serum metabolite profile in broiler chickens. *Food Funct.* 9:3776–3787.
- Wang, Y., L. Xia, T. Guo, C. Heng, L. Jiang, D. Wang, J. Wang, K. Li, and X. Zhan. 2020. Research Note: metabolic changes and physiological responses of broilers in the final stage of growth exposed to different environmental temperatures. *Poult. Sci.* 99:2017–2025.
- Wills-Karp, M. 2000. Trophic slime, allergic slime. *Am. J. Resp. Cell. Mol.* 22:637–639.
- Wood, T. 1986. Physiological functions of the pentose phosphate pathway. *Cell. Biochem. Funct.* 4:241–247.
- Yehudai-Ofir, D., I. Henig, and T. Zuckerman. 2020. Aberrant B cells, autoimmunity and the benefit of targeting B cells in chronic graft-versus-host disease. *Autoimmun. Rev.* 19:102493.
- Ylikahri, R. 1979. Metabolic and nutritional aspects of xylitol. Pages 159–180 in *Advances in Food Research*. Elsevier.
- Youn, Y., I. K. Sung, and I. G. Lee. 2013. The role of cytokines in seizures: interleukin (IL)-1 β , IL-1Ra, IL-8, and IL-10. *Korean J. Pediatr.* 56:271.